Progress In Electromagnetics Research C, Vol. 91, 173–183, 2019

A Compact Universal Antenna Design for UHF RFID Handheld Reader

Waleed A. Ahmed, Quanyuan Feng*, Zhuang Xiong, and Muhammad K. Khan

Abstract—A compact wideband circularly polarized (CP) square slot antenna for universal ultra high frequency (UHF) RF identification (RFID) handheld reader applications is proposed, fabricated, and tested. The antenna is coplanar waveguide (CPW) fed by an inverted Z-shaped feeding line. By inserting four stubs in diagonal directions and two inverted T-shaped strips inside the square slot, broadband CP operation, wide axial ratio bandwidth, and good impedance matching are achieved. The measured < -10 dB impedance bandwidth is from 706 MHz to 1007 MHz (301 MHz, 35.1%). The measured 3-dB axial ratio (AR) is 427 MHz (745–1172 MHz, 44.5%). The maximum measured gain of the proposed antenna is 4.8 dBi. The proposed antenna has wide impedance bandwidth, wide axial ratio bandwidth, and small size. The dimensions of the antenna are only $120 \times 120 \times 1.6$ mm^3. The impedance bandwidth and AR bandwidth performances of the proposed antenna can easily cover the UHF RFID band as whole.

1. INTRODUCTION

Radio frequency identification (RFID) technology is a wireless communication that employs radio waves to exchange the information between a tag and a reader for tracking and identification purposes. Nowadays, RFID in ultra high frequency (UHF) becomes a very popular technology used in several applications, such as access control system and supply chain management [1, 2]. Generally, an RFID system comprises an RFID tag with a chip and RFID reader device. The reader device with an antenna sends radio wave signal to RFID tag and receives a modulated signal from it to be processed. The RFID reader antenna with circular polarization (CP) is a preferred choice because RFID tags are normally randomly oriented, and RFID tag antenna is generally linearly polarized (LP) [3]. The frequency band assigned for UHF RFID applications is varied in different regions and countries. The full frequency range of UHF RFID is from 840 MHz to 960 MHz. Therefore, designing a reader antenna that covers the entire UHF RFID band with advantages of reduced cost as well as simplified implementation and configuration of RFID system will be beneficial [4]. According to some applications such as universal UHF RFID handheld applications, a reader antenna needs to have enough wide bands, perfect performance over the operating band, light weight, and compact size.

Over the past years, a number of reader antennas with different technics have been proposed as universal (840–960 MHz) UHF RFID reader antennas. An antenna is composed of two suspended truncated patches and a suspended microstrip line and fed by four probes which are connected to a microstrip line to produce a CP characteristic in [5]. In [6], radiation patch and parasitic radiation patch with air as dielectric layer and fed by two feeding lines connect to the main radiation patch tunable CP antenna based on ferrimagnetic substrate composed of top dielectric layer printed with rectangular radiation patch, middle ferrimagnetic layer, and bottom dielectric layer is studied in [7]. With a corner-truncated square driven patch with a stacked square parasitic patch and a microstrip

Received 25 January 2019, Accepted 9 March 2019, Scheduled 25 March 2019
* Corresponding author: Quanyuan Feng (fengquanyuan@163.com).
The authors are with the School of Information Science and Technology, Southwest Jiaotong University, Chengdu, China.

match stub suspended above the ground plane, the CP performance of this design can be optimized by adjusting the truncated driven patch with a parasitic patch is proposed in [8]. In [9], a patch antenna composed of three narrow slits is loaded at a corner truncated square patch using the technique of loading a corner truncated square patch antenna into an L-shaped ground plane to obtain broadband CP bandwidth is investigated. Two patches truncated on the corners to obtain the CP radiation, which are fed by horizontally meandered strip (HMS) feed technique and printed on an FR4 substrate are reported in [10]. However, these antenna designs have a large size, challenging fabrication, narrow impedance, and axial ratio bandwidths, and are not preferable to use in the UHF RFID handheld reader applications and applications which require compact antennas. A number of slot antennas with CP characteristic have been demonstrated such as stair-shaped slot antenna with a longitudinal slot etched at the middle part in [11]. In [12], a slot antenna with truncated corner and a grounded inverted L-shaped strip at the two opposite corners is studied. Recently, a planer broadband square slot antenna for UHF RFID system is reported in [13], and a compact UHF multiservice RFID reader antenna for near-field and far-field operations is proposed in [14]. However, both designed antennas have a relatively large size, narrow impedance bandwidth and axial ratio (AR) bandwidth, and does not cover the entire UHF RFID frequency range (840–960 MHz). Initial results for this solution were first presented in [15].

In this paper, we propose a compact CP slot antenna with wide impedance bandwidth, wide AR bandwidth, and compact size for universal UHF RFID handheld reader applications. The proposed antenna is fed by a coplanar waveguide (CPW) inverted Z-shaped feedline. By inserting four stubs in diagonal directions at slot corners and two inverted T-shaped strips into the square slot, good impedance matching, wide impedance bandwidth, and wide AR bandwidth are achieved. The overlapped operating bandwidth of the proposed antenna is 262 MHz (745–1007 MHz).

The following sections of this paper are organized as follows. Section 2 describes the antenna configuration. Parametric studies for significant parameters in the design are demonstrated in Section 3. Section 4 illustrates the antenna simulation and measurement results as well as a comparison in terms of $|S_{11}|$, 3-dB axial ratio, gain, and number of layers between the proposed antenna and other reader antennas mentioned in the open literature referred in this paper. A brief conclusion is presented in Section 5.

2. ANTENNA CONFIGURATION

The structure of the proposed antenna is shown in Figure 1. The proposed antenna is printed on an FR4 substrate (permittivity $\varepsilon_r = 4.4$ and loss tangent $\delta = 0.02$) with overall dimensions of $120\times120\times1.6\,\text{mm}^3$. Table 1 illustrates the optimal dimensions of the proposed antenna in detail. The proposed antenna comprises a square substrate of $120 \times 120\,\text{mm}^2$ with a square slot of $92 \times 92\,\text{mm}^2$ etched on the upper surface of the substrate, an inverted Z-shaped feedline on the lower surface of the substrate, four stubs in diagonal directions at the slot corners, and two inverted T-shaped strips inserted from the middle sides of the square slot towards the slot centre. The technic of CPW is used to obtain good impedance matching throughout the whole operating frequency band. One end of the matching $50\,\Omega$ microstrip feed line which has a width (d_1) of 1.7 mm and length of 14.5 mm is connected to the inverted Z-shaped feedline, while the other end is connected to the SMA connector. As shown in Figure 2, the design procedure of the proposed antenna can be described by three prototypes (Ant. A, Ant. B, and Ant. C). Note that, Ant. C is the proposed antenna in this paper. Figure 3 presents simulated reflection

Table 1. Dimensions of the proposed antenna.

Parameter	Value	Parameter	Value	Parameter	Value
L	120	L_5	46.0	W	120
L_1	24.0	d_1	1.7	W_1	4.0
L_2	4.0	d_2	0.5	W_2	20.0
L_3	35.0	d_3	5.0	W_3	28.5
L_4	92.0	d_4	8.8		

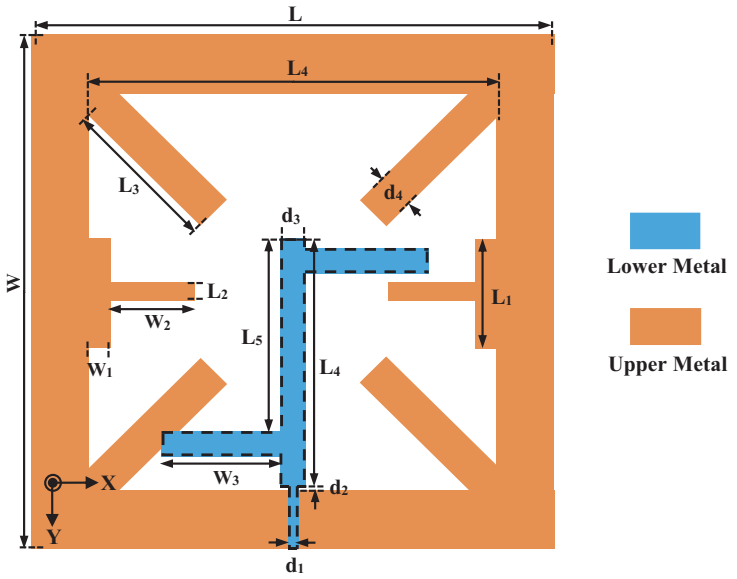

Figure 1. Geometry of the proposed antenna.

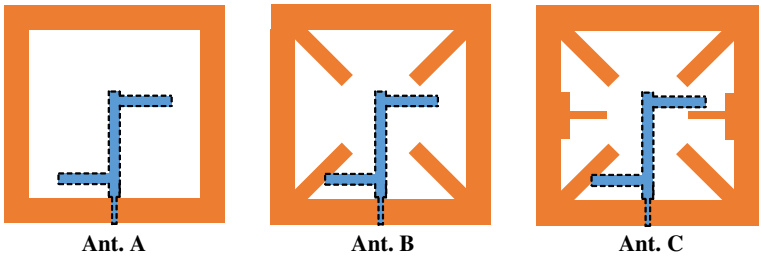

Figure 2. Design evolution of the proposed antenna.

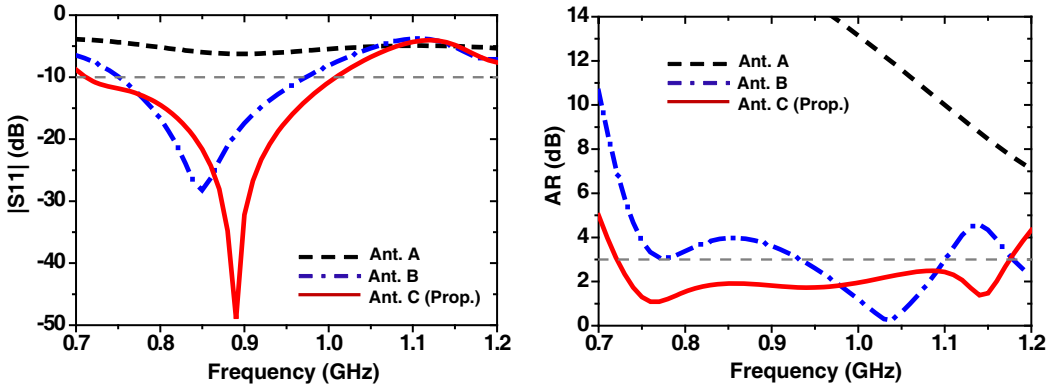

(a) (b)

Figure 3. Simulated results of antennas shown in Figure 2. (a) Reflection coefficient. (b) Axial ratio (AR).

coefficient $|S_{11}|$ and axial ratio results of the three antennas (Ant. A, Ant. B, and Ant. C (Prop.)). Ant. A is basic antenna and consists of an inverted Z-shaped feedline at the bottom centre of the substrate and a square slot at the top of the substrate. As shown in Figure 3, Ant. A has LP radiation and no CP radiation characteristics, and the impedance bandwidth is higher than -10 dB. In Ant. B, four stubs tuning in diagonal directions with length of L_3 and width of d_4 are added carefully to the structure

at the four corners of the square slot to realize CP radiation characteristics. The −10 dB reflection coefficient $|S_{11}|$ of Ant. B is from 752 to 973 MHz, and it covers the whole operating band of UHF RFID. However, the axial ratio of Ant. B is from 931 to 1101 MHz and does not cover the entire UHF RFID band (840–960 MHz). To obtain the proposed antenna (Ant. C), two inverted T-shaped strip lines with width of 4 mm and vertical stub length of 24 mm and horizontal stub length of 20 mm are insetted at the middle of the two sides of the square slot towards the slot centre to provide wide bandwidth and improve the total performance of the antenna in terms of the impedance and axial ratio bandwidths. Ant. C (Prop.) has a good impedance matching, good CP radiation characteristics, wide impedance bandwidth, wide AR bandwidth, and it covers the global UHF RFID band easily.

To explain the CP radiation for the proposed antenna, the simulated current distributions on the slot and feedline at four phase angles 0°, 90°, 180°, and 270° are depicted in Figure 4. As clearly seen in the figure, the current travels in clockwise direction as the phase angle increases by 90°, which generates a left-hand circular polarization (LHCP) radiation in the $+z$ direction. In contrast, the right-hand circular polarization (RHCP) radiation in the $+z$ direction can be achieved by reverse the x-axis direction of the two rectangular stubs of the feedline. Therefore, the proposed antenna has a dual circular polarization system. The simulated input impedance of the designed antenna is illustrated in Figure 5. As shown in this figure, the optimal values of both the real and imaginary parts of the input impedance (50 Ω for the resistance part and 0 Ω for the reactance part) at resonant frequency of 890 MHz are achieved in the proposed antenna.

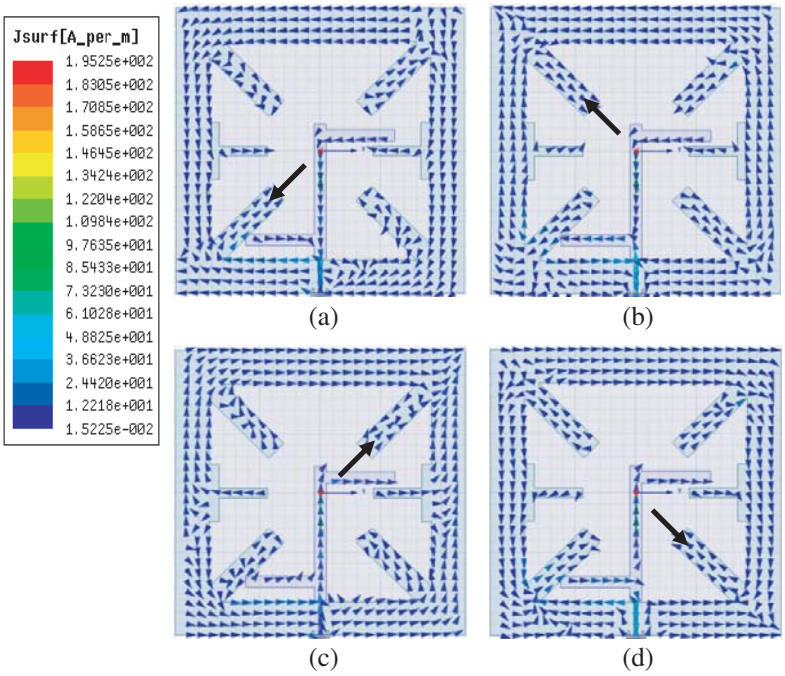

Figure 4. Distributions of the surface current at 0.9 GHz with four phase angles (a) 0°, (b) 90°, (c) 180°, and (d) 270°.

3. PARAMETRIC STUDIES

Different simulation results are obtained by using high-frequency structure simulator (HFSS version 13). Several simulation results for significant parameters are realized to illustrate the influence of these parameters on both the S_{11} bandwidth and AR bandwidth of the proposed antenna. Note that only one parameter in this paper is tuned, and the other parameters are fixed.

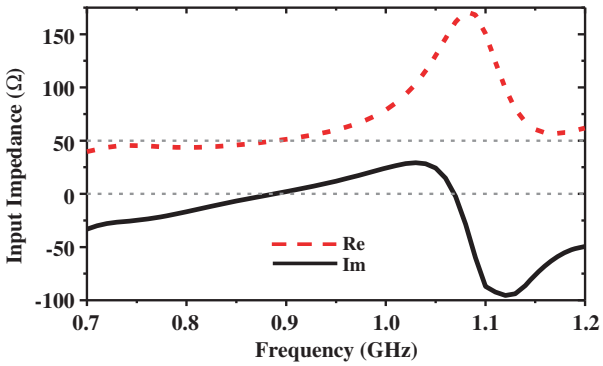

Figure 5. Simulated input impedance of the proposed antenna.

3.1. Influence of the Length L_3

Figure 6 depicts the influence of tuning the length L_3 on the S_{11} and AR bandwidths. As shown in Figure 6(a), the end frequency of the reflection coefficient band is decreased when the value of L_3 increases. In addition, the impedance matching decreases when L_3 is increased except at $L_3 = 35$ mm (proposed). On the other hand, the influence of L_3 on AR bandwidth is demonstrated in Figure 6(b). The AR band is increased when L_3 increases till 35 mm (proposed). After that, the AR band is decreased and distorted at $L_3 = 37$ mm, 39 mm, and 41 mm. It is worth noting that parameter L_3 is a significant parameter in this design, and the value of L_3 can reconfigure both the end frequency band of the S_{11} band and AR band significantly. Consequently, the value of L_3 is optimized carefully.

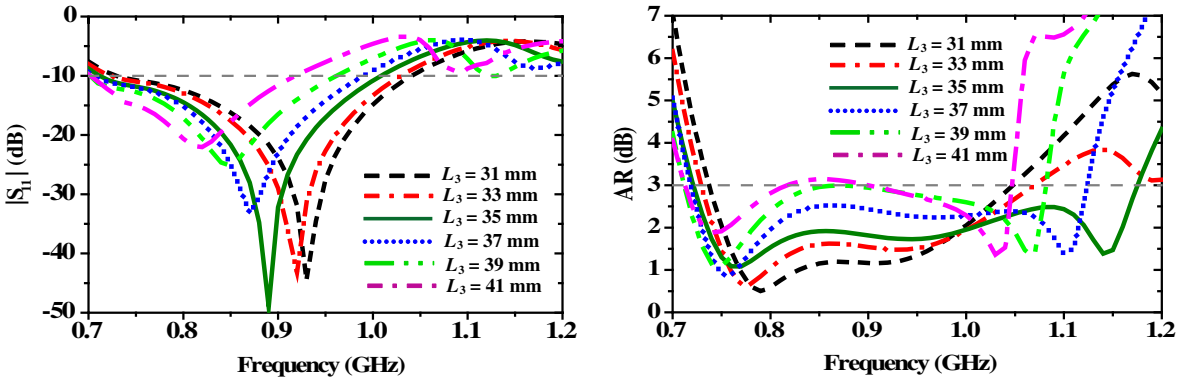

Figure 6. (a) Reflection coefficient $|S_{11}|$ and (b) AR when L_3 tuned.

3.2. Influence of the Length W_3

Figure 7 illustrates the effect of tuning the length W_3 on the antenna performance (S_{11} and AR bandwidths). When the value of W_3 is increased, the frequency band of S_{11} and the resonant frequency are shifted to lower frequencies, as shown in Figure 7(a). The effect of W_3 on AR bandwidth is shown in Figure 7(b). The 3-dB AR bandwidth becomes wider to cover the entire UHF RFID range when W_3 is increased from 26.5 mm to 28.5 mm. Then, the 3-dB AR bandwidth is divided to two bands ($W_3 = 29.5$ mm). The first band covers the entire UHF RFID range, but the S_{11} band at this value of W_3 does not cover the full UHF RFID bandwidth. The best results of S_{11} and AR bandwidths are at $W_3 = 28.5$ mm (Prop.). It is worth mentioning that parameter W_3 is one of the significant parameters in the design, and it can reconfigure the antenna performance. The value of parameter W_3 is chosen properly.

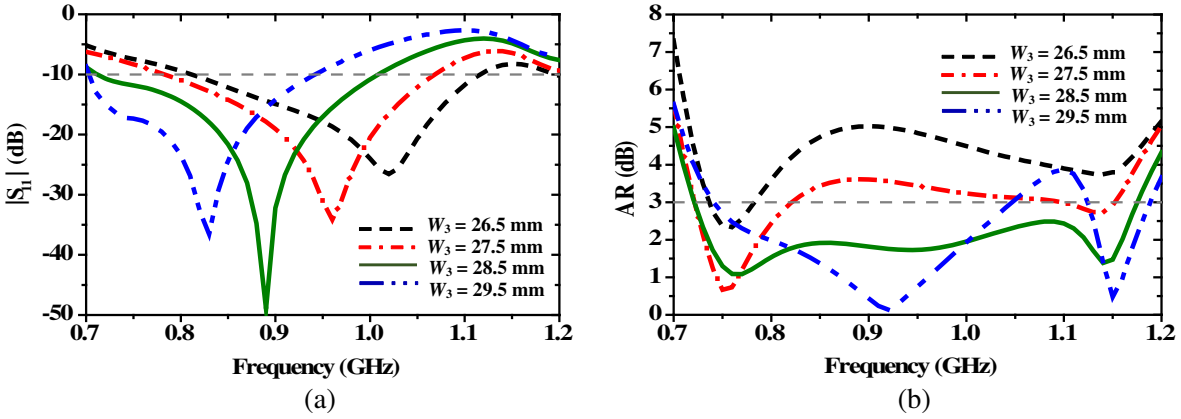

Figure 7. (a) Reflection coefficient $|S_{11}|$ and (b) AR when W_3 tuned.

3.3. The Effect of W_2

The influence of length W_2 on AR bandwidth is depicted in Figure 8. According to Figure 8, the end frequency of AR bandwidth shifts to lower frequencies when W_2 is increased. It is noted that W_2 can control the end frequency of AR bandwidth.

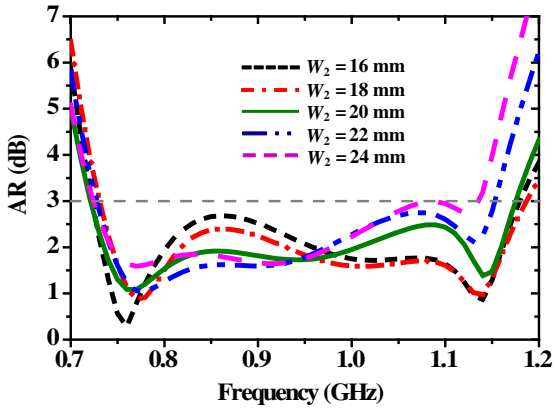

Figure 8. The axial ratio bandwidth when W_2 tuned.

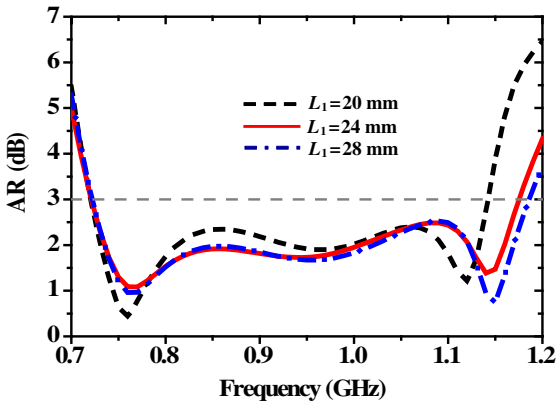

Figure 9. The axial ratio bandwidth when L_1 tuned.

3.4. The Influence of L_1

Figure 9 exhibits the effect of tuning length L_1 on AR bandwidth of the proposed antenna. It is noted that the end frequency of the AR band increases when L_1 is increased. Besides, parameter L_1 can control the end frequency of the AR bandwidth without any influence on start frequency.

4. SIMULATION AND MEASUREMENT RESULTS

Ansoft High-Frequency Structure Simulator (HFSS) is employed to obtain simulation results, and An E5071C performance network analyzer is used to measure the antenna reflection coefficient. The comparison of the simulated and measured antenna reflection coefficients $|S_{11}|$ is shown in Figure 10(a). The simulated and measured bandwidths evaluated at -10 dB reflection coefficient $|S_{11}|$ are 295 MHz (712–1007 MHz, 34.3%) and 301 MHz (706–1007 MHz, 35.1%), respectively. The simulated resonant frequency is at 890 MHz whereas the measured one is at 900 MHz. The measured reflection coefficient

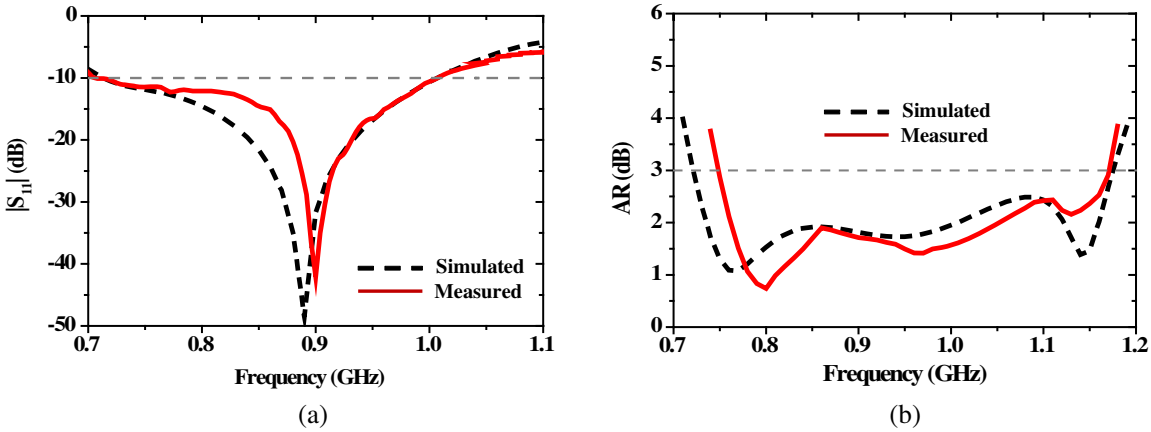

(a) (b)

Figure 10. Simulated and measured results of (a) reflection coefficient $|S_{11}|$ and (b) axial ratio of the proposed antenna.

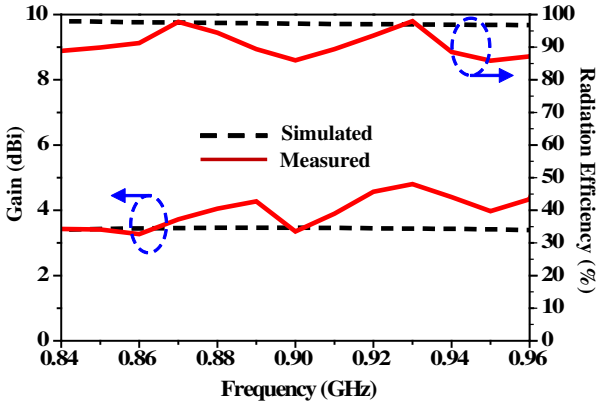

Figure 11. Simulated and measured radiation efficiency and gain across the UHF RFID band for the proposed antenna.

performance agrees well with the simulation result. Figure 10(b) illustrates the simulated and measured performance results of 3-dB AR. The simulated 3-dB axial ratio bandwidth is 456 MHz (721–1177 MHz, 48.0%), whereas the measured one is 427 MHz (745–1172 MHz, 44.5%). The simulated and measured results of axial ratio mostly agree well with each other.

The far-field performances of the proposed antenna are measured in an anechoic chamber by using a SATIMO measurement system. The simulated and measured antenna radiation efficiencies and gains are shown in Figure 11. The proposed antenna has minimum measured radiation efficiency higher than 85%. The maximum measured gain of the proposed antenna is 4.8 dBi at 930 MHz. The slight discrepancy between the measured and simulated gains and efficiencies can be mainly attributed to the tolerance of fabrication process. The simulated and measured radiation patterns of the proposed antenna at 840 MHz, 900 MHz, and 960 MHz (start, middle, and end frequency of universal UHF RFID band, respectively) for x-z and y-z planes are depicted in Figure 12. The radiation pattern results show bidirectional radiation characteristics. The simulated radiation patterns agree well with the measured ones.

Figure 13 illustrates the reading-range measurement of the CP proposed antenna which is performed by rotating Alien dipole-liked tag AZ9662 (operating frequency 860–960 MHz, reading range about $0.01 \sim 6$ m) with dimensions of 70 mm $\times$ 17 mm along the directions of $\pm z$-axis. To detect a UHF RFID tag, the proposed reader antenna is connected to UHF RFID reader module (JRM2030) with low utput power of 27 dBm and operating frequency 902–928 MHz. The measured results show that the maximum reading-range in free space is maintained between 2.95 and 3.45 meters.

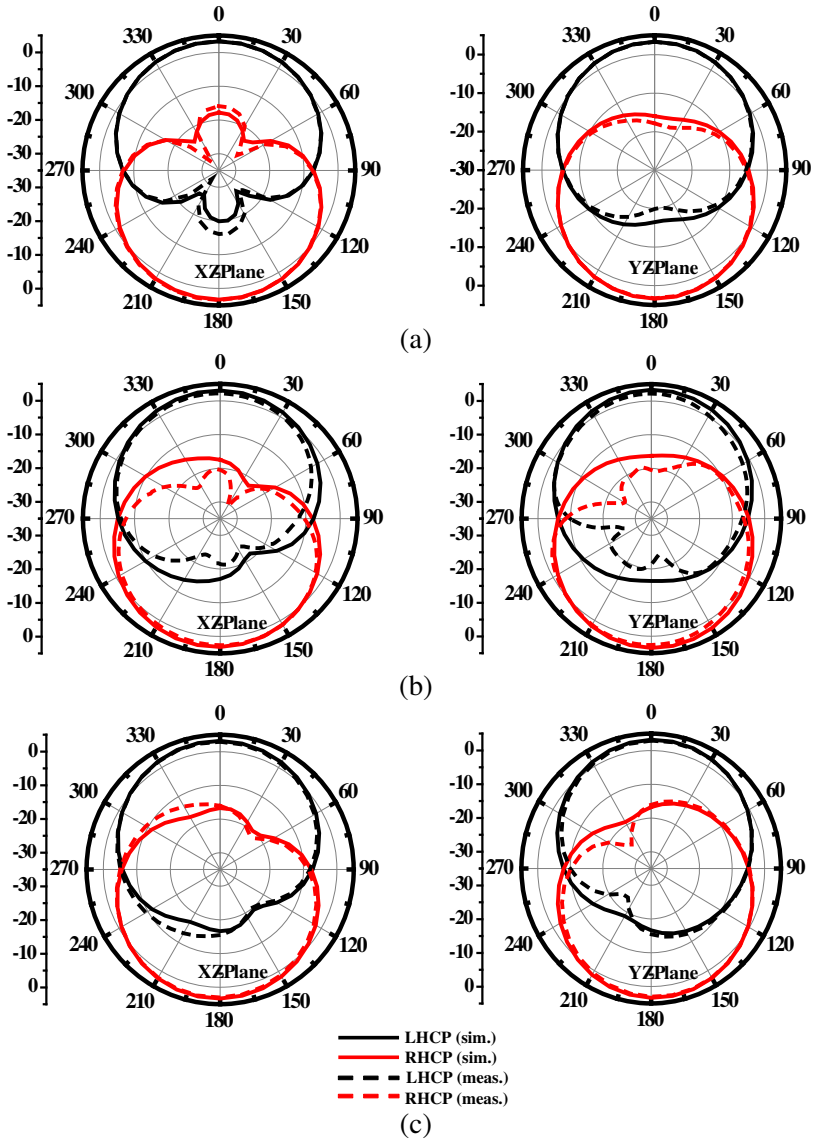

Figure 12. Antenna radiation patterns at: (a) 840 MHz. (b) 900 MHz. and (c) 960 MHz.

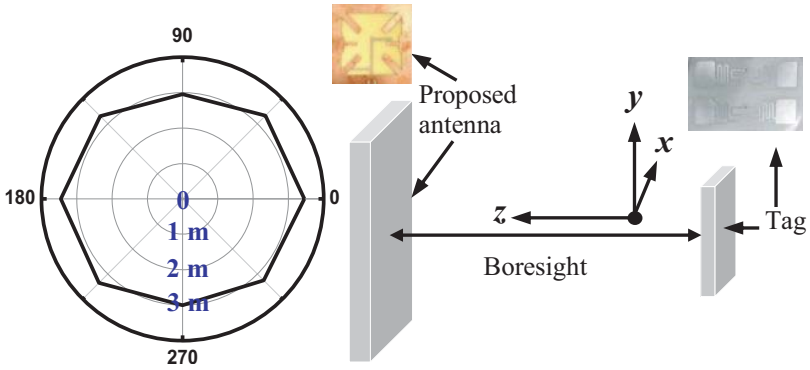

Figure 13. Measured reading ranges for tag rotating in $\pm z$-axis.

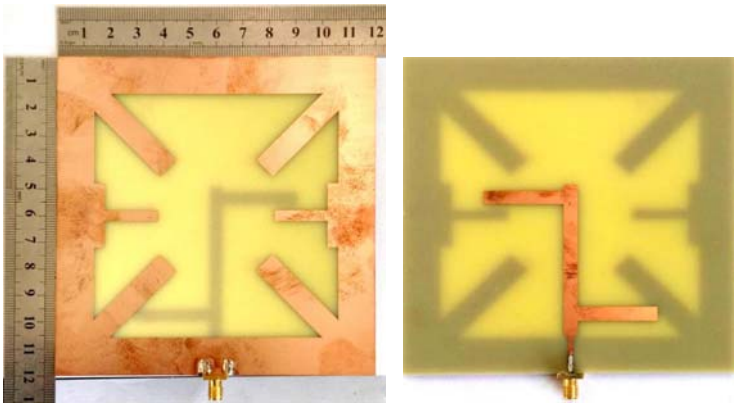

(a) (b)

Figure 14. Photographs of the proposed antenna. (a) Top view. (b) Bottom view.

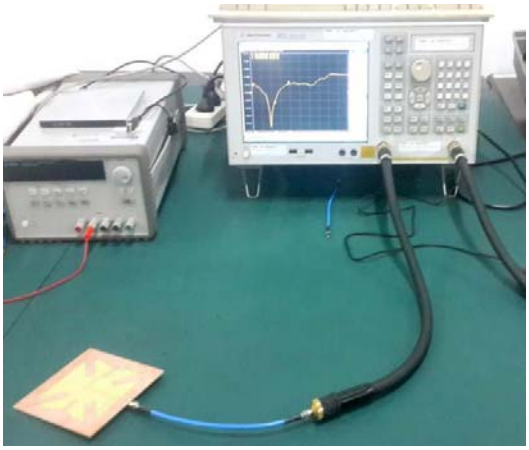

Figure 15. Photograph of the proposed antenna under test using Agilent E5071C VNA.

Table 2. Antenna performance comparison.

Ant.	−10 dB reflection coefficient BW (MHz)	3-dB axial ratio BW (MHz)	Max. Gain (dBi)	Dimensions ($L \times W \times H$) mm^3	No. of layers
Ref. [4]	194 768–962	141 816–957	9.8	$250 \times 250 \times 35$	3
Ref. [5]	203 760–963	146 818–964	8.3	$250 \times 250 \times 35$	3
Ref. [6]	180 800–980	100 860–960	9.7	$341 \times 341 \times 26.6$	3
Ref. [8]	126 834–960	120 840–960	9.0	$240 \times 240 \times 28$	3
Ref. [9]	440 685–1125	150 836–986	8.6	$250 \times 250 \times 60$	2
Ref. [10]	225 758–983	121 838–959	8.6	$250 \times 250 \times 26.5$	4
Ref. [13]	142 860–1002	166 857–1023	6.8	$126 \times 121 \times 0.8$	1
Ref. [14]	110 815–925	35 835–870	5.5	$83 \times 83 \times 1.6$	1
Proposed	**301** **706–1007**	**427** **745–1172**	**4.8**	$120 \times 120 \times 1.6$	**1**

Clear photographs of both the top view and bottom view of the proposed antenna are displayed in Figure 14. A photograph of experimental setup to measure the reflection coefficient of fabricated antenna using Agilent E5071C VNA is shown in Figure 15.

Table 2 illustrates a comparison between the proposed antenna and other CP antennas designed as universal UHF RFID reader antennas. As clearly seen in the table, the proposed antenna has the merits of wide S_{11} bandwidth, wide AR bandwidth, and smaller volume than all other antennas presented in Table 2. The designed antennas in [4, 6, 10] have a large volume, and not suitable for

handheld reader applications, composed of more than two layers of ground plane, and their overlapping operating bandwidths do not cover the entire universal UHF RFID range (840–960 MHz). Reader antennas proposed in [5, 8, 9] cover the entire universal UHF RFID band. However, these antennas have a large volume and not appropriate for UHF RFID handheld applications. Although the antennas in [13, 14] have a compact size and can be integrated in handheld device, these antennas do not cover the range from 840 MHz to 960 MHz.

5. CONCLUSION

In this paper, a compact wideband CP slot antenna for universal UHF RFID applications has been presented, fabricated, and tested. By inserting four tuning stubs in diagonal directions and two inverted T-shaped strips inside the square slot, wide S_{11} and wide axial ratio bandwidths are achieved. The proposed antenna has a measured -10 dB reflection coefficient of 301 MHz (706–1007 MHz), measured 3-dB AR bandwidth of 427 MHz (745–1172 MHz), a dual circular polarization system, and maximum measured peak gain of 4.8 dBi. The measurement results agree well with the simulated ones. The structure of the proposed antenna has a planar single-layer and is simple. The proposed antenna has overall size of $120 \times 120 \times 1.6$ mm^3, and it is a good candidate for universal UHF RFID handheld reader applications.

ACKNOWLEDGMENT

This work is supported by the Key Project of the National Natural Science Foundation of China under Grant 61531016, 61831017 and the Sichuan Provincial Science and Technology Important Projects under Grant 2018GZ0139, 18ZDZX0148, and 2018GZDZX0001.

REFERENCES

1. Wang, B., "A compact antenna design for UHF RFID applications," *Progress In Electromagnetics Research Letters*, Vol. 53, 83–88, 2015.
2. Wu, T., H. Su, L. Gan, H. Chen, J. Huang, and H. Zhang, "A compact and broadband microstrip stacked patch antenna with circular polarization for 2.45-GHz mobile RFID reader," *IEEE Antennas and Wireless Propagation Letters*, Vol. 12, 623–626, 2013.
3. Pan, C.-Y., C.-C. Su, G.-J. Wu, and J.-Y. Jan, "Circularly polarized monopole antenna using short-circuited sleeve strip for UHF RFID reader," *Microwave and Optical Technology Letters*, Vol. 56, 957–961, 2014.
4. Liu, X., Y. Liu, and M. M. Tentzeris, "A novel circularly polarized antenna with coin-shaped patches and a ring-shaped strip for worldwide UHF RFID applications," *IEEE Antennas and Wireless Propagation Letters*, Vol. 14, 707–710, 2015.
5. Chen, Z. N., X. Qing, and H. L. Chung, "A universal UHF RFID reader antenna," *IEEE Transactions on Microwave Theory and Techniques*, Vol. 57, 1275–1282, 2009.
6. Li, J., Y. Huang, Y. Wang, Q. Zhang, G. Wen, and H. Zhang, "Wideband high gain circularly polarized UHF RFID reader antenna," *2016 IEEE Conference on Antenna Measurements & Applications (CAMA)*, 1–3, 2016.
7. Wu, K., G. Wen, Y. Huang, J. Li, and H. Sun, "Universal UHF RFID reader antenna based on the ferrimagnetic slab with tunable operating frequency," *2014 IEEE International Conference on Communication Problem-Solving (ICCP)*, 60–63, 2014.
8. Fu, S., C. Li, S. Fang, and Z. Wang, "Low-cost single-fed circularly polarized stacked patch antenna for UHF RFID reader applications," *2016 Progress In Electromagnetic Research Symposium (PIERS)*, 2031–2034, Shanghai, China, Aug. 8–11, 2016.
9. Sim, C., Y. Hsu, and G. Yang, "Slits loaded circularly polarized universal UHF RFID reader antenna," *IEEE Antennas and Wireless Propagation Letters*, Vol. 14, 827–830, 2015.

10. Wang, Z., S. Fang, S. Fu, and S. Jia, "Single-fed broadband circularly polarized stacked patch antenna with horizontally meandered strip for universal UHF RFID applications," *IEEE Transactions on Microwave Theory and Techniques*, Vol. 59, 1066–1073, 2011.
11. Wang, C. and C. Chen, "CPW-fed stair-shaped slot antennas with circular polarization," *IEEE Transactions on Antennas and Propagation*, Vol. 57, 2483–2486, 2009.
12. Shen, Y., C. L. Law, and Z. Shen, "A CPW-fed circularly polarized antenna for lower ultra-wideband applications," *Microwave and Optical Technology Letters*, Vol. 51, 2365–2369, 2009.
13. Lu, J.-H. and S.-F. Wang, "Planar broadband circularly polarized antenna with square slot for UHF RFID reader," *IEEE Transactions on Antennas and Propagation*, Vol. 61, 45–53, 2013.
14. Pakkathillam, J. K., M. Kanagasabai, and M. G. N. Alsath, "Compact multiservice UHF RFID reader antenna for near-field and far-field operations," *IEEE Antennas and Wireless Propagation Letters*, Vol. 16, 149–152, 2017.
15. Abdelrahim, W. and Q. Feng, "Wideband circularly polarized slot antenna for universal UHF RFID reader," *2018 International Conference on Microwave and Millimeter Wave Technology (ICMMT)*, 1–3, Chengdu, China, 2018.